Applied Thermal Engineering 62 (2014) 553–559

Contents lists available at ScienceDirect

Applied Thermal Engineering

journal homepage: www.elsevier.com/locate/apthermeng

Experimental results of a 10 kW high temperature thermochemical storage reactor based on calcium hydroxide

Matthias Schmidt [a,*], Christoph Szczukowski [a], Christian Roßkopf [b], Marc Linder [b], Antje Wörner [b]

[a] German Aerospace Center – DLR e.V., Institute of Technical Thermodynamics, Linder Höhe, 51147 Köln, Germany
[b] German Aerospace Center – DLR e.V., Institute of Technical Thermodynamics, Pfaffenwaldring 38, 70569 Stuttgart, Germany

HIGHLIGHTS

- Multifunctional test bench and indirect operated reactor developed and in operation.
- Proof of principal for a 10 kW, 20 kg calcium hydroxide thermochemical storage reactor.
- Several charge and discharge cycles were performed at adjustable storage temperatures.

ARTICLE INFO

Article history:
Received 21 June 2013
Accepted 12 September 2013
Available online 30 September 2013

Keywords:
Thermochemical heat storage
High temperature
Gas–solid reaction
Calcium hydroxide
Calcium oxide
Pilot plant

ABSTRACT

One promising possibility to store thermal energy is by means of reversible gas solid reactions. In this context, the endothermal dehydration of calcium hydroxide ($Ca(OH)_2$) to calcium oxide (CaO) is a well known, cycle stable reaction able to store heat at temperatures above 410 °C and pressures above 0.1 bar. Additionally, the storage material itself is a widely available low cost raw material which allows for low cost thermal energy storage capacities. Therefore, a multifunctional test bench for thermochemical storage reactors has been developed and set into operation. Simultaneously an indirect operated reactor for ~20 kg $Ca(OH)_2$ was designed, manufactured and integrated into the test bench. Within this work the charge and discharge characteristics of the reactor concerning possible limitations due to heat and mass transfer were studied experimentally. Thereby, the possibility to store and release the heat of reaction at an adjustable temperature level was demonstrated in a technical relevant scale. The storage material remained stable and showed no degradation effects after ten cycles.

1. Introduction

Efficient thermal energy storage systems for high temperatures at reasonable costs are essential for the economic success of concentrated solar power and increase efficiency through the recovery of waste heat in industrial processes. An overview on the wide variety of thermal storage methods and possible applications is given by Dincer et al. [1]. The thermochemical storage of heat using gas–solid reactions offers several advantages compared to conventional sensible and latent heat storage methods: storage densities are higher, thermal losses are minimal and heat can be transformed within a certain temperature range through the variation of the partial pressure of the gaseous reactant. Additionally, application of different reaction systems with adjustable equilibrium temperatures offers the possibility to adapt the storage temperatures to the respective process needs.

So far, salt hydrates have been characterized as suitable candidates for heat storage in the temperature range between 20 and 200 °C [1–3] while several metal hydroxide systems are considered to cover a temperature range between 250 and 600 °C [4,5]. However, especially regarding the high temperature applications, available literature deals in general with thermal analysis measurements [7–9] of a few gram sample or investigations in small scale laboratory reactors with a maximum of 400 g of storage material [10–14]. The behavior of a 20 kg reaction bed in an indirect operated reactor is still unclear and therefore experimentally investigated in this work.

Due to the good availability at low cost and its favorable temperature range, previous work at DLR focused on the reversible dissociation reaction of $Ca(OH)_2$:

* Corresponding author. Tel.: +49 22036014091.
E-mail address: matthias.schmidt@dlr.de (M. Schmidt).

1359-4311/$ – see front matter © 2013 Elsevier Ltd. All rights reserved.
http://dx.doi.org/10.1016/j.applthermaleng.2013.09.020

$$Ca(OH)_2(s) + \Delta H_{reaction} \leftrightarrow CaO(s) + H_2O(g) \quad (1)$$

Complete reversibility, cycling stability and sufficiently fast reaction kinetics of the system have been demonstrated in thermal gravimetric analysis studies [8]. No degradation effects have been observed after 100 performed cycles. Consequently, the material can be considered as long term stable, if side reactions during handling or storage of larger bulks can be avoided. Furthermore, the high reaction enthalpy of about 100 kJ/mol and the adjustable temperature range between 410 °C and 520 °C make the system a promising candidate e.g. for application in concentrated solar power plants [6].

However, besides the thermochemical characterization of the storage material, efficient and upscalable reactor concepts need to be developed. In a directly operated reactor the heat transfer fluid (HTF) flows through the reaction bed offering good heat transfer but high pressure drop. In order to avoid high pressure drop, the HTF can be physically separated from the storage material by an integrated heat exchanger. Disadvantageous with this indirectly operated reactor concept is that heat transfer into the reaction bed is poor, due to the generally low thermal conductivity of the storage material bulk of 0.1 W/mK.

Schaube et al. demonstrated the feasibility of the directly operated reactor concept in laboratory scale [11]. However, because of the high pressure drop of the powder bed an upscaling of this concept is considered uneconomical. Therefore an indirectly operated reactor was designed and manufactured. Simultaneously a multifunctional test bench capable to investigate different thermochemical reactors was build and set in operation at DLR [15].

In order to investigate the reaction material in larger scale, this study focuses on hydration and dehydration cycles of this indirectly operated reactor in pilot scale (20 kg of CaO). The reached temperatures of the HTF and the bed are measured for both cycle directions and the amount of stored and released heat is balanced. The coherency between the applied steam partial pressure and the temperatures reached in the reaction bed is shown experimentally and corresponds to the theoretically calculated values. In principle, a peak power mode, where the maximum thermal load was observed and a nominal power mode, where a smaller load was supplied for an extended time, were realized for the discharge of the storage reactor.

2. Experimental setup

2.1. Reactor concept

For the experiments in this work an indirectly operated reactor based on a plate heat exchanger concept (see Fig. 1) was manufactured and integrated into the test bench. Characteristic numbers of weight, volume and permissible temperatures are given in Table 1. All parts of the reactor are made from a high temperature alloy (see Table 1). Based on prior operating experience with a laboratory reactor [11], we do not expect corrosion problems.

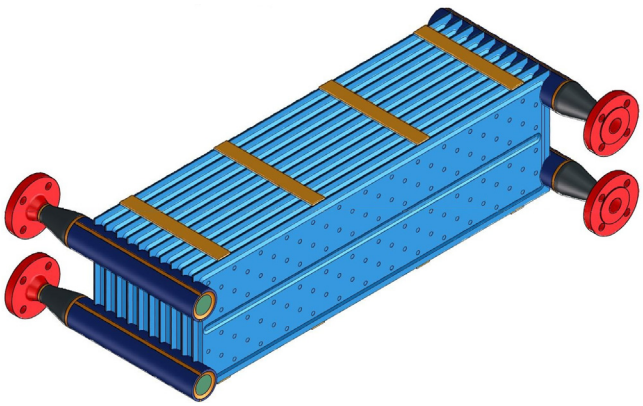

Fig. 1. Schematic of the indirectly operated reactor [16].

Table 1
Specifications of the reactor.

Material (reactor and thermoshelves):	1.4404 – X2CrNiMo 17-12-2
Metal weight:	145 kg
Reaction bed dimensions:	45 l (~25 kg $Ca(OH)_2$) 20 × 200 × 850 mm (10 channels)
Max. permissible temperature:	600 °C
Max. permissible pressure:	Reaction gas side: 0.1–2.5 bar HTF side: 0–5.0 bar
Thermoshelves:	1.5 × 250 × 850 mm (10 shelves) 4.25 m^2 total heat transfer area
Power:	$P_{Nominal} = 5\ kW_{th}$ $P_{max} = 10\ kW_{th}$
HTF mass flow:	$\dot{m} = 0.00283–0.0531$ kg/s

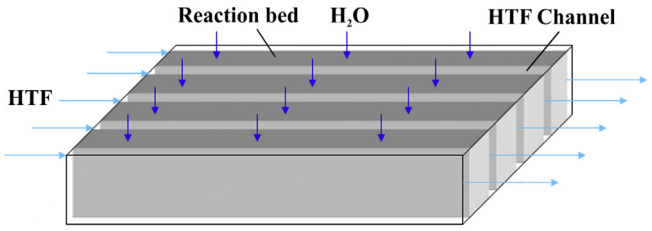

Fig. 2. Schematic of the cross flow design of the pilot reactor [15].

On the right side the HTF, in this case air, enters the reactor at the two flange connections. The HTF flows through ten spot-welded thermoshelves which distribute the flow uniformly over the reactor height (Fig. 1). Between the thermoshelves the storage material is placed in the 20 mm wide channels (Fig. 2). Along the length of the reactor the HTF takes up or releases heat to or from the powder bed and leaves the reactor at the opposite site.

The water vapor enters or leaves the reaction chamber through an inlet pipe placed in the center of the cover plate. A 30 mm gap between the inlet and the surface of the bulk ensures uniform distribution of the reaction gas. This cross-flow arrangement between the HTF and the reaction gas allows for sufficient heat exchange area along the length of the reactor while the reaction gas only has to overcome a short distance through the reaction bed to the bottom of the reactor (Fig. 2). Thus, the pressure drop over the reaction bed is minimal and a uniform equilibrium temperature over the entire bed volume can be expected.

To observe the reaction front and to identify possible limitations due to heat and mass transfer of the gaseous reactant 21 thermocouples (type K, class 1, 2 mm) are installed inside the reaction bed. Fig. 3 shows the position of the thermocouples in the reactor. 13 thermocouples ($T_1 - T_{13}$) are installed in the central channel along the direction of flow in various depths. Additionally, one thermocouple is installed in each of the 8 parallel channels ($T_{14} - T_{21}$).

2.2. Material sample

For the experiments in this study, calcium hydroxide by HeidelbergCement Group is used. It is a commercial product, called “lime hydrate ip500”, which is mainly applied in building industry for the mortar production but also in food and paper industries. It is produced by slaking calcium oxide with water.

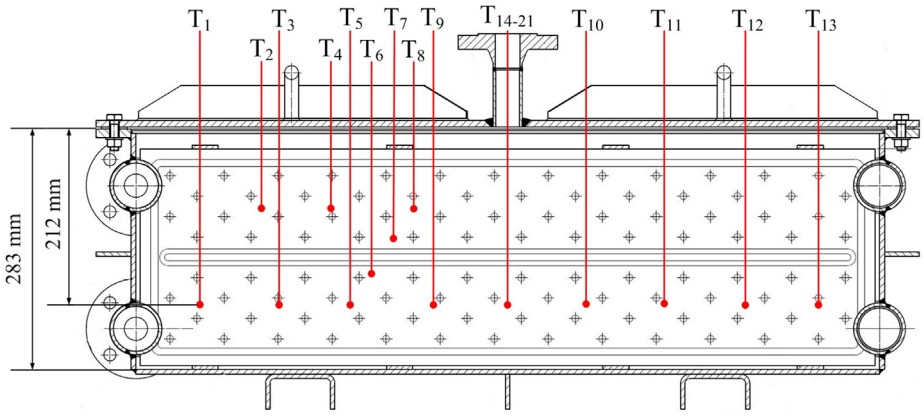

Fig. 3. Side view of the cross-section and position of the thermocouples in the reaction bed.

Referring to the datasheet provided by the company the purity of the material is about 97%. The true density of $Ca(OH)_2$ is 2240 kg/m^3, whereas it is 3300 kg/m^{3}of CaO. Due to its small particle size (d50 = 5 μm) the powder has a very cohesive character. Hence, the porosity varies from 0.5 to 0.8 according to the infilling process. For the investigations within this work, the reactor is filled with a mass of approximately 20 kg of $Ca(OH)_2$ (Fig. 4). This value can deviate up to 100 g due to unavoidable mass losses of the fine powder during infilling. Based on a bed volume of 45 l (Table 1) this results in a bulk density of ρ_{bed} = 445.2 kg/m^3. The heat capacity depends on the temperature and is between 1200 and 1600 J/kg K for $Ca(OH)_2$ and 700 and 900 J/kg K for CaO. The thermal conductivity depends on the porosity of the reaction bed and is about 0.1 W/m K [8].

2.3. Test bench

The reactor has been integrated into the test bench for thermochemical storage systems at DLR. A process flow diagram of the experimental setup is shown in Fig. 5.

Fig. 4. Reactor filled with 20 kg of $Ca(OH)_2$.

The test bench consists of three main units, the supply of the HTF at demanded temperatures and mass flows, the reaction gas supply and the cooling and disposal of the gas stream. The HTF supply and cooling unit is in principle independent of the type of reactor being integrated and the investigated storage material.

2.3.1. HTF supply unit

A compressor conveys ambient air with a maximum volume flow of 160 nm^3/h at 10 bar. To ensure a continuous availability of the air flow a buffer tank is installed with a capacity of 1 m^3 air and a maximum pressure of 10 bars. Via two mass flow controllers (Bronkhorst, digital flow controller, ±0.5%) the HTF flow can be adjusted in a range of 8–160 nm^3/h at a pressure of up to 5 bar. Subsequent the HTF can be heated up to 700 °C in electrical heaters. Downstream the HTF enters the reactor, delivering or taking up the heat of reaction.

2.3.2. Reaction gas supply unit

For the reaction gas supply an additional evaporator/condenser unit, shown in Fig. 5, was developed. A tube bundle heat exchanger (HEX) with a casing volume of 8.5 l is filled with 2 l of distilled water. A vacuum pump is connected in order to evacuate the system down to an absolute pressure of 10 mbar to enable a pure water vapor atmosphere. The water level is constantly measured by a fluid level sensor (Vegaflex 65, coaxial measuring probe, ±2 mm). Via a thermostatic bath the temperature of the thermo fluid running in

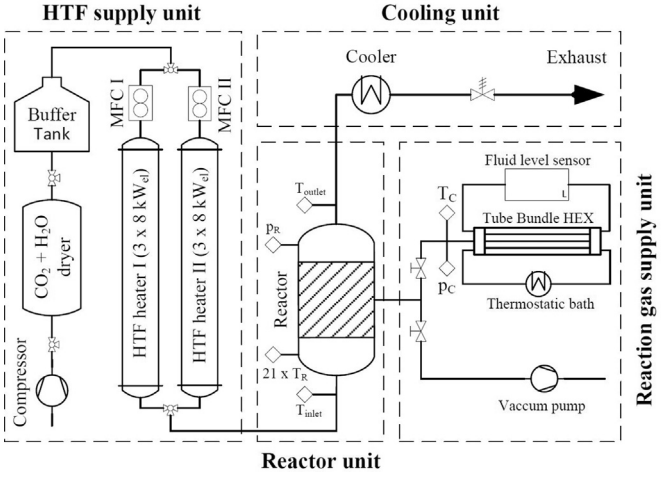

Fig. 5. Process flow diagram of the test bench.

the tubes can be set between −50 °C and 250 °C. While decomposition of the storage material takes place in the reactor a certain condensation temperature can be adjusted in the HEX. Thus the released vapor is condensed in the reaction gas supply unit at constant condensation pressure.

To discharge the storage reactor a certain evaporation temperature can be adjusted by the thermostatic bath. Thus steam is generated in the HEX, flows into the reactor and enables the hydration reaction at constant pressure. Based on the measured change of the water level in the HEX, the overall rate of conversion in the reactor can be determined. The conversion in percentage can be calculated as the ratio of the amount of water absorbed or released during the reaction to the theoretical amount of water based on the stoichiometric reaction:

$$c[\%] = \frac{\Delta m_{H_2O,HEX}}{m_{H_2O,stoichiometric}} \quad (2)$$

The reactor is filled with an amount of 20 kg $Ca(OH)_2$. According to equation (1) and the molar masses of the reactants, the theoretical amount of water is calculated to $m_{H2O,stoichiometric} = 4.871$ kg.

2.3.3. Cooling and disposal of HTF stream

During discharge, temperatures of up to 600 °C can be reached at the reactor outlet. This hot gas stream needs to be cooled down before control valves can be placed and the gas stream can be directed into the chimney. Therefore, a gas water heat exchanger was designed to cool down the HTF stream from 600 °C to 300 °C. After the cooler a pressure valve is placed to adjust the gas pressure corresponding to the gas velocity in the internal heat exchanger channels.

2.4. Experimental methodology

2.4.1. Equilibrium temperature and operation mode of the reactor

During charging or discharging the present water vapor pressure, which is adjusted by the temperature setting in the evaporator/condenser unit, defines the temperature at which the reaction takes place. Fig. 6 shows the theoretical coherence between the water vapor pressure and the equilibrium temperature for the $Ca(OH)_2$/CaO reaction system based on the values of Barin [17].

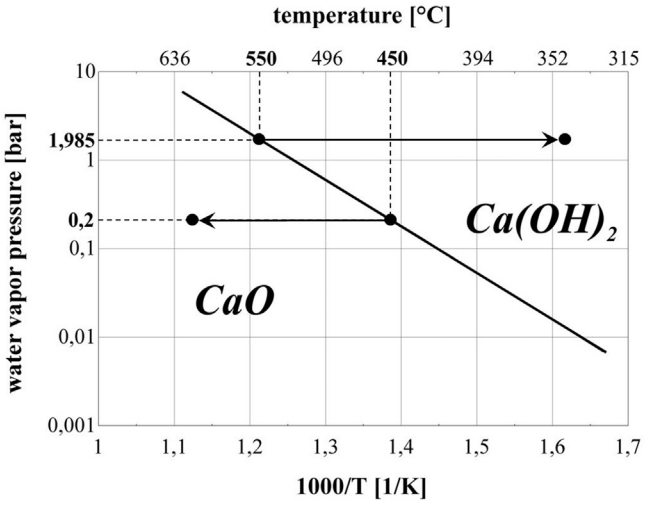

Fig. 6. Equilibrium line for the $Ca(OH)_2$ reaction system calculated with values of Barin [17].

Different studies have already dealt with the experimental determination of the equilibrium temperature of $Ca(OH)_2$/CaO-reaction system. Samms and Evans determined an equilibrium temperature of 510 °C at a water vapor pressure of 1 bar. Based on their measurements the equilibrium in the pressure range of 1–50 bar can be calculated as [18]:

$$\ln\left(\frac{p_{H_2O}}{[bar]}\right) = -\frac{11375}{T[K]} + 14.574 \quad (3)$$

For operation of the thermochemical heat storage, a detailed understanding of this equilibrium line is necessary. In case of the discharging process, the heat has to be removed from the reaction bed. Therefore, the reaction temperature has to be higher than the inlet temperature of the HTF. This can be reached by adjusting the water vapor pressure that, according to Fig. 6, defines the maximum reaction temperature. Additionally, the evolution of the HTF temperature along the reactor is important. As soon as the HTF reaches the equilibrium temperature of the reaction, a further heat exchange between the reaction bed and HTF is not possible – consequently the reaction stops. Therefore, based on the interaction between HTF temperature, its mass flow and the pressure of the reaction gas, different operation modes of the reactor can be realized (e.g. full power, or nominal power, compare Section 3.2).

2.4.2. Dehydration procedure

Before the dehydration gets initiated, the setup is preheated by the HTF and additional electrical resistance heaters to 400 °C until it reaches isothermal conditions. The volume flow of the HTF is kept constant for the whole cycle. In order to obtain a high temperature difference between the temperature of the HTF and the reaction bed, the system is evacuated and a constant temperature of 5 °C is applied in the condenser of the gas supply unit. To initiate the reaction, the temperature of the HTF is increased to 590 °C and kept constant until the conversion of the material is complete.

2.4.3. Hydration procedure

Before initiating the hydration, the setup is preheated to 350 °C until isothermal conditions are reached. Throughout the experiment, the air volume flow and inlet temperature is kept constant at 350 °C. In order to achieve a high discharge temperature the evaporator is heated to a temperature of 120 °C producing a water vapor atmosphere at the corresponding steam pressure of 1.985 bar. According to Fig. 6 this corresponds to an equilibrium temperature of about 550 °C. The reaction is then initiated by opening the valve between the reactor and the evaporator (compare Fig. 5).

3. Results and discussion

3.1. Dehydration of $Ca(OH)_2$

Fig. 7 shows the temperature profile of the air inlet ($T_{air;in}$) and outlet temperature ($T_{air;out}$), the temperatures T_1, T_5, T_{11}, T_{13} (compare Fig. 3) in the reaction bed, as well as the conversion rate during dehydration for an air volume flow of 150 nm^3/h. After isothermal conditions are reached ($T_{air,in} = 400$ °C), the dehydration is initialized by increasing the air inlet temperature. After about 60 min, the air inlet temperature reaches 590 °C and remains constant during the whole experiment. In the beginning the air outlet temperature and the bed temperatures (T_1, T_5, T_{11}, T_{13}) rise with the same gradient as the air inlet temperature. The continuous heat input causes sensible warming of the bed. After about 40 min the bed is at 450 °C which is the corresponding equilibrium temperature for the present 0.2 bar water vapor atmosphere (compare

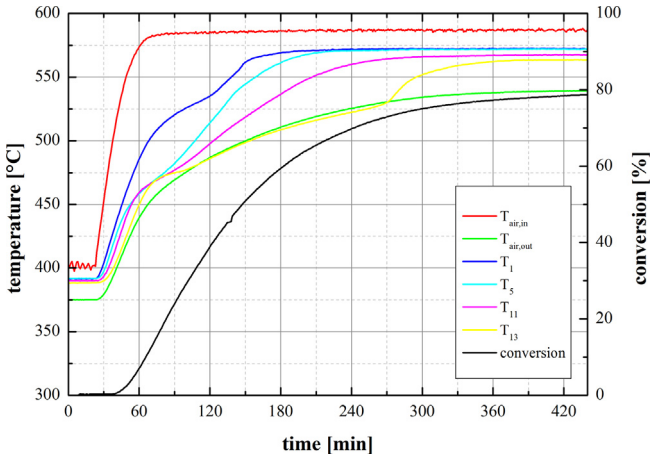

Fig. 7. Dehydration at maximum air volume flow: temperatures and conversion profile.

Fig. 6). From there on the endothermic dehydration of the $Ca(OH)_2$ with the release of water vapor starts indicated by a drop in the gradient of the bed temperatures. At the same time the conversion starts to increase. The rate of conversion is high in the beginning and drops slightly towards the end of the experiment since less material is present to react. After about 6 h the bed reaches a constant temperature of 570 °C as well as a constant water level, thus the dehydration cycle is completed. Overall, a conversion of 77% of the material in the reactor was determined. This value is calculated with the measured change of the water level and the method explained in Section 2.3.2.

3.2. Hydration at peak power mode

Fig. 8 shows the temperature profiles of the air inlet and outlet temperature, the bed temperatures and the conversion during the hydration procedure. In order to reach the peak power of the reactor the maximum air volume flow of 150 nm^3/h is supplied. The reaction is initiated by opening the valve between reactor and evaporator, whereby water vapor at 1.985 bar flows into the reaction chamber. The temperatures in the reaction bed increase immediately above 500 °C due to the exothermal hydration reaction being initiated. The reaction heat released is also indicated by the air outlet temperature that increases by about 125 K to a temperature of 475 °C within 14 min the reaction bed temperatures reach 500 °C at the entrance area of the reactor (T_1) only for a short time since the HTF inlet cools the bed immediately. In the center part of the reactor (T_5, T_{11}) around 530–540 °C are reached. And towards the outlet of the HTF (T_{13}) the temperature of the bed reaches the equilibrium temperature of ~550 °C and decreases slowly. Consequently, due to the decreasing reaction, the air outlet temperature begins to decay shortly after reaching the maximum temperature level of 475 °C. After 50 min the outlet temperature underruns 450 °C and decreases until it reaches 350 °C after 100 min Fig. 8 shows additionally the conversion during the hydration. At the end of the experiment an overall conversion of 78% was determined. Compared with the dehydration cycle (Section 3.1), the same amount of material took part in the formation as in the dissociation reaction.

3.3. Hydration at nominal power mode

In order to investigate the influence of the flow rate on the storage reactor the volume flow of the air was halved to 75 nm^3/h compared to peak power mode. The basic idea was to reach an increased operation time with constant, nominal power output due to a reduced heat transfer of the HTF (nominal operation mode).

Fig. 9 shows the air inlet and outlet temperature, the bed temperatures and the conversion rate while hydration in nominal power mode. Immediately after the water vapor is supplied, heat is released from the reactor. This is reflected in an increase in the air outlet temperature within a few minutes of about 135 K to a temperature level of about 485 °C. The temperatures in the reaction bed show also an immediate rise to about 520 °C. Due to the good cooling at the entrance area of the reactor, the reaction temperature T_1 begins to decrease already 5 min after reaching the maximum temperature level. At the same time, in the sectors along the air flow direction, the temperatures T_5, T_{11} and T_{13} still increase due to the pressure equalization in the system after opening the valve between evaporator and reactor. The equilibrium temperature of 546 °C corresponding to the water vapor pressure of 1.985 bar (Fig. 6) is reached 13 min after starting the reaction and can be kept constant for around 35 min at thermocouple T_{13}. This indicates that in consequence of the reduced heat transfer due to the reduced HTF flow rate, the reaction time is extended. Thus, the equilibrium temperature can be maintained for an extended time span. This is also reflected in a slower drop in the air outlet temperature (Fig. 8), which starts to decrease 5 min after the maximum temperature of 485 °C is reached and stays above 450 °C for 65 min due to the gradual temperature drop along the flow direction (T_1, T_5, T_{11}, T_{13}) it

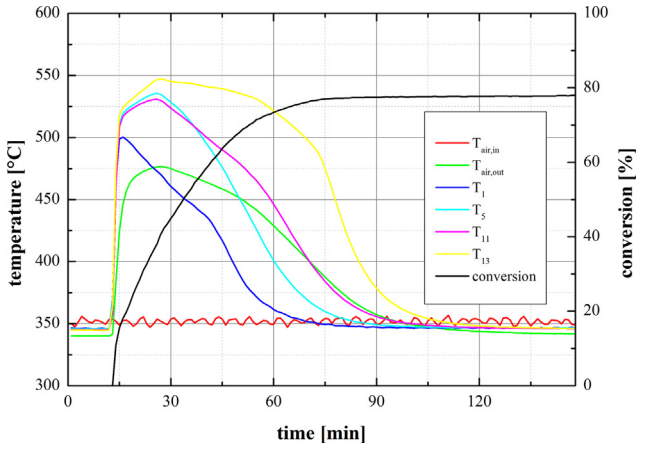

Fig. 8. Hydration at maximum air volume flow: temperatures and conversion profile.

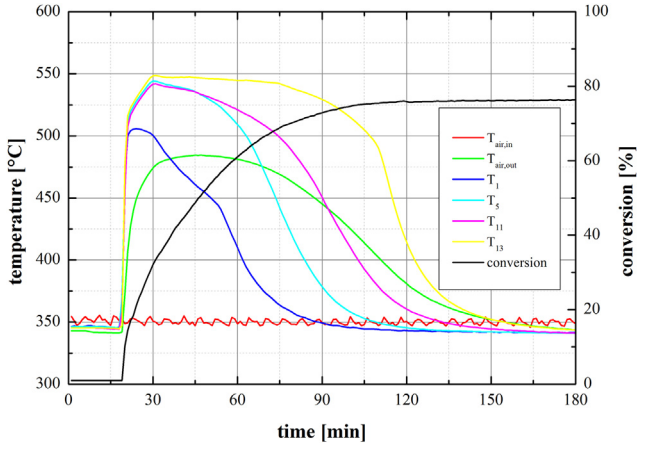

Fig. 9. Hydration at nominal air volume flow: temperatures and conversion profile.

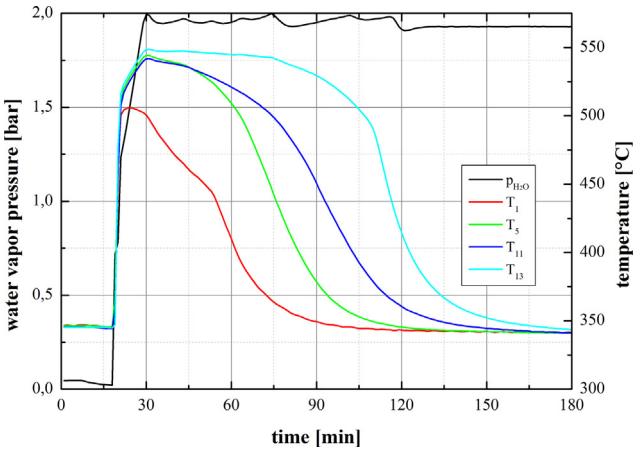

Fig. 10. Water vapor pressure and bed temperatures at nominal power mode.

is evident that a reaction front moves through the bed length – from the entrance area to the outlet area of the reactor.

After about 150 min the air outlet temperature drops to 350 °C again, indicating that the hydration cycle is complete. In accordance to the experiments shown above, an overall conversion of 76.5% was measured.

3.4. Equilibrium temperature and reaction gas distribution within the bed

Fig. 10 shows the water vapor pressure during the hydration in nominal power mode and the reaction temperatures at the bottom of the reaction bed (compare Fig. 3). During the whole experiment the water vapor pressure is kept constant at about 1.985 bar. According to equation (3) this corresponds to an equilibrium temperature of 546 °C. The reaction temperatures measured at thermocouples T_5, T_{11} and T_{13} reach a maximum temperature of 542–549 °C which is in very good agreement with the results of Samms and Evans [18]. Based on the measured reaction temperatures, a sufficient gas distribution within the bed can be assumed: firstly, the water vapor distributes in the entire bed within seconds – measured by the increased temperature due to the triggered reaction. Secondly, the bed temperatures (T_5, T_{11}, T_{13}) reach the theoretically calculated equilibrium temperature for the applied steam partial pressure. Since these temperature sensors are located at the opposite side of the water vapor inlet, a significant pressure loss for the reaction gas along the depth of the bed can be excluded.

3.5. Implications for the process application

The performed experiments demonstrate the possibility to operate the reactor with an adjustable power output and outlet temperature. During the discharge in nominal mode (Fig. 9) the reaction bed temperature remains constant for a period of time. Consequently a constant outlet temperature is achievable as longs as enough material is present to react and the heat transfer from the bed to the HTF is sufficient. Such a storage system is especially advantageous for applications where the process demands a constant inlet temperature and a fluctuating heat source (sun or waste heat stream) is present.

The heat recovery efficiency of the proposed reaction system depends mainly on the process and on the integration principle. It is obvious that the enthalpy of vaporization is an energetic effort and has to be taken into account if steam needs to be generated. In the worst case scenario the heat recovery efficiency of the system is reduced to 60% if the enthalpy of vaporization (40 kJ/mol) has to be taken from the enthalpy of reaction and the condensation enthalpy during charging cannot be used. On the other hand, if water vapor is available, e.g. in form of waste steam in industrial processes, even an upgrade of thermal energy is possible (heat transformation). Moreover, since in order to recover the enthalpy of reaction of 100 kJ/mol at 500 °C water vapor at around 100 °C is needed. A direct operation of a steam turbine cycle that partially uses low grade steam to drive the chemical reaction could be possible.

Therefore, any technical and economical evaluation of a thermochemical storage reactor demands a detailed energy and exergy performance analysis in respect to the process parameters. Besides the incorporation of the heat fluxes an integration of the reaction gas into the process in order to reach a high overall efficiency is necessary. Consequently, a performance analysis demands a detailed understanding of the process, the development of integration strategies as well as modeling of the entire system. These topics are currently addressed and will be covered in future works.

4. Conclusions

In this work the experimental results of an indirectly operated thermochemical storage reactor for 20 kg $Ca(OH)_2$ are presented. Several dehydration and hydration cycles were performed in order to study the charge and discharge characteristics of the storage reactor.

Based on the performed experiments the feasibility to store heat thermochemically with the $Ca(OH)_2$/CaO reaction system in technically relevant scale (10 kW) could be demonstrated. The dehydration was performed at 450 °C and the rehydration at about 550 °C. Reversible conversion of 77% of the material with no degradation effects after 10 cycles was determined. In comparison to earlier thermogramivetric analysis [6], the conversion is clearly reduced. This is currently under investigation but most likely related to carbonization of the material during handling.

Through the variation of the HTF mass flow the power output of the reactor could be adjusted and controlled. Two different operation modes of the storage reactor were realized. In the peak power mode a maximum thermal power of 7.5 kW_{th} was reached and the air outlet temperature could be kept above 450 °C for 35 min in nominal power mode a constant heat release at 3 kW_{th} was realized for an extended period. In this case the air outlet temperature could be kept above 450 °C for 75 min and a reaction front along the reaction bed has been observed.

Future work with this type of reactor will deal with the investigation of different charging and discharging temperatures as well as the optimization of the overall conversion of the material.

Acknowledgements

This work has been partially funded by the Federal Ministry of Economics and Technology in the frame of the CWS project (0327468A).

References

[1] I. Dincer, M.A. Rosen, Thermal Energy Storage. Systems and Applications, second ed., Wiley, 2002.
[2] M. Molenda, M. Bouché, M. Linder, M. Blug, J. Busse, A. Wörner, Thermochemical energy storage for low temperature applications: materials and first studies in a gas-solid reactor, in: Proceedings of 12th Int. Conference on Energy Storage (Innostock), Lleida, Spain, 2012.
[3] F. Bertsch, B. Mette, S. Asenbeck, H. Kerskes, H. Müller-Steinhagen, Low temperature chemical heat storage – an investigation of hydration reactions, in: Proceedings of 11th Int. Conference on Thermal Energy Storages (Effstock), Stockholm, Sweden, 2009.

[4] V.M. van Essen, Characterization of salt hydrates for compact seasonal thermochemical storage, in: Proceedings of the 3rd Int. Conference of Energy Sustainability (ASME), San Francisco, USA, 2009.
[5] Y. Kato, R. Takahashi, T. Sekiguchi, J. Ryu, Study on medium-temperature chemical heat storage using mixed hydroxides, Int. J. Refrig. 32 (4) (2009) 661–666.
[6] F. Schaube, A. Wörner, R. Tamme, High temperature thermochemical heat storage for concentrated solar power using gas–solid reactions, J. Solar Energy Eng. 133 (3) (2011) 031006–031006-7.
[7] M.N. Azpiazu, J.M. Morquillas, A. Vazquez, Heat recovery from a thermal energy storage based on the $Ca(OH)_2$/CaO cycle, Appl. Therm. Eng. 23 (6) (2003) 733–741.
[8] F. Schaube, L. Koch, A. Wörner, H. Müller-Steinhagen, A thermodynamic and kinetic study of the de- and rehydration of $Ca(OH)_2$ at high H_2O partial pressures for thermo-chemical heat storage, Thermochim. Acta 538 (2012) 9–20.
[9] F. Schaube, A. Wörner, H. Müller-Steinhagen, High temperature heat storage using gas-solid reactions, in: Proceedings of 11th Int. Conference on Thermal Energy Storages (Effstock), Stockholm, Sweden, 2009.
[10] J. Cot-Gores, A. Castell, L.F. Cabeza, Thermochemical energy storage and conversion: a-state-of-the-art review of the experimental research under practical conditions, Renewable Sustainable Energy Rev. 16 (2012) 5207–5224.
[11] F. Schaube, A. Kohzer, J. Schütz, A. Wörner, H. Müller-Steinhagen, De- and rehydration of $Ca(OH)_2$ in a reactor with direct heat transfer for thermochemical heat storage. Part A: experimental results, Chem. Eng. Res. Des. 91 (5) (2013) 856–864.
[12] M. Zamengo, J. Ryu, Y. Kato, Magnesium hydroxide – expanded graphite composite pellets for a packed bed reactor chemical heat pump, Appl. Therm. Eng. (2013), http://dx.doi.org/10.1016/j.applthermaleng.2013.04.045.
[13] H. Ogura, T. Yamamoto, H. Kage, Effects of heat exchange condition on hot air production by a chemical heat pump dryer using $CaO/H_2O/Ca(OH)_2$ reaction, Chem. Eng. J. 86 (2002) 3–10.
[14] K. Darkwa, Thermochemical energy storage in inorganic oxides: an experimental evaluation, Appl. Therm. Eng. 18 (6) (1998) 387–400.
[15] P. Schmidt, M. Bouché, M. Linder, A. Wörner, Pilot plant development of high temperature thermochemical heat storage, in: Proceedings of 12th Int. Conference on Energy Storage (Innostock), Lleida, Spain, 2012.
[16] Drawing of a high temperature plate heat exchanger, 2012. Available: www.deg-engineering.de. (accessed 05.08.13).
[17] I. Barin, Thermochemical Data of Pure Substances, VCH Verlagsgesellschaft, 1995.
[18] A.C. Samms, B.E. Evans, Thermal dissociation of $Ca(OH)_2$ at elevated pressures, J. Appl. Chem. 18 (1968) 5–8.

Nomenclature

C: conversion [%]
g: gaseous
$H_{reaction}$: heat of reaction [kJ/mol]
HEX: heat exchanger
HTF: heat transfer fluid
m: mass [kg]
M: molar mass [g/mol]
MFC: mass flow controller
s: solid
$T_1 - T_{21}$: temperature in the bulk [°C]
T_C: temperature condenser [°C]
T_{inlet}: air temperature reactor inlet [°C]
T_{outlet}: air temperature reactor outlet [°C]
T_R: temperature reactor [°C]
$\dot{V}$: volume flow
p_C: pressure condenser [bar]
p_{H2O}: water vapor pressure [bar]
p_R: pressure reactor [bar]
ρ: density [kg/m^3]
ρ_{bed}: bulk density [kg/m^3]
ε: porosity

Subscripts
C: condenser
max: maximum
n: norm
R: reactor
th: thermal